

Consistency analysis for the performance of planar detector systems used in advanced radiotherapy

Kanan Jassal¹, Biplob Sarkar¹, Anusheel Munshi¹, Shilpi Roy¹, Sayan Paul¹, Bidhu Kalayan Mohanti¹, Tharmar Ganesh¹, Arun Chougule², Kanupriya Sachdev³

¹Department of Radiation Oncology, Fortis Memorial Research Institute, Gurgaon, India

²Department of Radiological Physics, SMS Medical College and Hospital, Jaipur, India

³Department of Physics, Malaviya National Institute of Technology, Jaipur, India

Received September 23, 2014; Revised December 12, 2014; Accepted December 14, 2014; Published Online December 18, 2014

Original Article

Abstract

Purpose: To evaluate the performance linked to the consistency of a-Si EPID and ion-chamber array detectors for dose verification in advanced radiotherapy. **Methods:** Planar measurements were made for 250 patients using an array of ion chamber and a-Si EPID. For pre-treatment verification, the plans were generated on the phantom for re-calculation of doses. The γ -evaluation method with the criteria: dose-difference (DD) $\leq 3\%$ and distance-to-agreement (DTA) ≤ 3 mm was used for the comparison of measurements. Also, the central axis (CAX) doses were measured using 0.125cc ion chamber and were compared with the central chamber of array and central pixel correlated dose value from EPID image. Two types of statistical approaches were applied for the analysis. Conventional statistics used analysis of variance (ANOVA) and unpaired t-test to evaluate the performance of the detectors. And statistical process control (SPC) was utilized to study the statistical variation for the measured data. Control charts (CC) based on an average (\bar{X}), standard deviation (\bar{S}) and exponentially weighted moving averages (EWMA) were prepared. The capability index (C_{pm}) was determined as an indicator for the performance consistency of the two systems. **Results:** Array and EPID measurements had the average gamma pass rates as $99.9\% \pm 0.15\%$ and $98.9\% \pm 1.06\%$ respectively. For the point doses, the 0.125cc chamber results were within $2.1\% \pm 0.5\%$ of the central chamber of the array. Similarly, CAX doses from EPID and chamber matched within $1.5\% \pm 0.3\%$. The control charts showed that both the detectors were performing optimally and all the data points were within $\pm 5\%$. EWMA charts revealed that both the detectors had a slow drift along the mean of the processes but was found well within $\pm 3\%$. Further, higher C_{pm} values for EPID demonstrate its higher efficiency for radiotherapy techniques. **Conclusion:** The performances of both the detectors were seen to be of high quality irrespective of the radiotherapy technique. Higher C_{pm} values for EPID indicate its higher efficiency than array.

Keywords: a-Si EPID Dosimetry; γ – Analysis; Statistical Process Control; Capability Index

Introduction

In recent years, volumetric intensity-modulated arc therapy (VMAT), static intensity modulated radiotherapy (s-IMRT) and dynamic intensity modulated radiotherapy (d-IMRT) has been adopted as the preferred option for the treatment due to high dose conformity for the target and achieving high dose gradients around the periphery of the target, thus sparing the organs at risk (OAR).¹⁻⁵ These advanced techniques utilize the ability of multileaf collimator (MLC) to generate the arbitrary shapes and computer algorithm to develop treatment plan by optimization strategies such as simulated annealing.⁶⁻⁸ This has led to an immense need for quality control in such complex planning and delivery of treatment plans. In the clinical setting, it is highly recommended due to the fact that these errors could lead to fatal consequences.⁹⁻¹⁰

The planar measurements in phantom geometry provide an evaluation of the MLC and linear accelerator performance for a patient specific plan. For the quantitative analysis, the combination of dose-difference (DD) and distance-to-agreement (DTA) is used to provide a single numerical quantity known as the gamma (γ) index.¹¹⁻¹³ It is a measure of disagreement between calculated and measured planar region that does not match to the acceptance criteria and indicate the calculation quality in the region that pass the acceptance criteria. In order to explore the stability and fluctuations in the process of quality assurance for patient specific IMRT / VMAT plans, the newer concept of statistical process control¹⁴⁻¹⁷ can be applied. It is a popular tool amongst the modern quality control techniques.¹⁸⁻¹⁹ Besides positional verification²⁰⁻²¹ and quality control of linac^{19,22-23, 24}, several studies have validated a-Si EPID for patient specific dosimetry.

Corresponding author: Kanan Jassal; Department of Radiation Oncology, Fortis Memorial Research Institute, Gurgaon, India.

Cite this article as: Jassal K, Sarkar B, Munshi A, Roy S, Paul S, Mohanti BK, Ganesh T, Chougule A, Sachdev K. Consistency analysis for the performance of planar detector systems used in advanced radiotherapy. *Int J Cancer Ther Oncol* 2015; 3(1):030110. DOI: 10.14319/ijcto.0301.10

The present study quantifies the efficiency and consistency of a-Si EPID as a planar detector when compared with ion-chamber array over a large group of patients (N=250). The primary goal of this study was to explore a metrics/method for evaluating consistency of the quality assurance (QA) devices in a reliable manner. We have applied traditional as well as the newer tools of statistical process control (SPC) to the measurements undertaken prospectively on the modern radiotherapy techniques using a ion chamber array, a-Si EPID (for planar measurements) and ionization chamber (for point dose measurements) on linear accelerators. The purpose of utilizing control charts (CC) in this work as a tool in radiotherapy was to monitor the performance of the detectors (equipment) and delivery of radiotherapy technique (process) for patient-by-patient basis in advanced techniques.

Methods and Materials

Treatment planning, optimization and pre-treatment verification procedures

Patients (N=250) were divided into four categories: brain ($n_1=62$), head and neck ($n_2=62$), thorax ($n_3=63$) and pelvis ($n_4=63$). These patients were treated with advanced radiation therapy techniques viz. s-IMRT or d-IMRT or VMAT using 6 MV photon beams available at our center from September 2012 to January 2014. For our study purpose, we planned all the 250 patients thrice: first for s-IMRT, second for d-IMRT and third for VMAT planning. Treatment planning for s-IMRT, d-IMRT and VMAT were performed with Monaco version 3.20.01. This system utilizes virtual energy fluence (VEF) as a radiation source in combination with X-Ray Voxel Monte Carlo (XVMC) method for dose computation. Kawrakow *et al.* developed VMC as a fast dose calculation engine for electron beams²⁵, and later on it was extended to photon beams and was named as XVMC.²⁶ The process of optimization requires constraints as an objective function for regions of interest (ROI): target and organs-at-risk (OAR) volumes. For the pre-selected beams angles/arcs, system optimizes fluence distribution and generates MLC segments based on beamlets. Further, the segment weight optimization (SWO) algorithm optimizes the number of segments to achieve the desired dose distribution. The dose calculation cube voxel size and the statistical uncertainty of the XVMC dose calculation used in this study were $3 \times 3 \times 3 \text{ mm}^3$ and 1%, respectively.

For the patient specific pretreatment quality assurance for s-IMRT, d-IMRT and VMAT were performed systematically twice with 2D array (PTW, Freiburg) and a-Si EPID.²¹⁻²⁴ These detectors worked in the integrated mode, so the fluence delivered with each and every beam and segment was accumulated in a single frame. The measured fluence was compared with the TPS calculated fluence. The clinical tolerance,

$$\Delta_{Array}(\%) = 100 - (\gamma\%)_{Array} \quad \text{and}$$

$\Delta_{EPID}(\%) = 100 - (\gamma\%)_{EPID}$ as per ICRU-83 was taken as $< \pm 3\%$ irrespective of the anatomical site and the type of the technique used.

Statistical analysis: traditional and statistical process control

In the present work the conventional statistic and the statistical process control as the modern quality management tool was applied, to analyze the consistency of a-Si EPID and ion-chamber array detector systems. The data characterization included the identification of the statistical distribution that fits the data appropriately. Data points were plotted as histogram and were checked for its goodness of fit (GoF) to a normal distribution. The (Jarque-Bera) JB statistics²⁸ was selected since it has a two-sided goodness of fit test, suitable when the sample is tested against the unknown population and also the population parameters are required to be estimated. It is specifically designed as the alternative to the Pearson's system of distribution. The JB test evaluates the null hypothesis (H_0) that the all two set of samples Δ_{Array} and Δ_{EPID} follow a normal distribution and quantifies the differences between the 2 samples and normal distribution using the sample skewness and kurtosis. The test statistics JB is defined as $JB = \frac{n}{6} \left[s^2 + \frac{1}{4}(k-3)^2 \right]$ Where, n is the number of

observations, s is the sample skewness and k is the sample kurtosis. Skewness and kurtosis are evaluated as

$$s = \frac{\hat{\mu}_3}{\hat{\sigma}_3} = \frac{\frac{1}{n} \sum_{i=1}^n (x_i - \bar{x})^3}{\left(\frac{1}{n} \sum_{i=1}^n (x_i - \bar{x})^2 \right)^{3/2}}$$

$$k = \frac{\hat{\mu}_4}{\hat{\sigma}_4} = \frac{\frac{1}{n} \sum_{i=1}^n (x_i - \bar{x})^4}{\left(\frac{1}{n} \sum_{i=1}^n (x_i - \bar{x})^2 \right)^2}$$

where, $\hat{\mu}_3$ and $\hat{\mu}_4$ are the estimates of third and fourth central moments, respectively, \bar{x} is the sample mean, and $\hat{\sigma}^2$ is the estimate of the second central moment, the variance.

The difference between the detectors used for different modern radiotherapy techniques was evaluated using hypothesis testing. The t-test analysis was considered an appropriate test for judging the significance of a sample mean, in case when population variance is not known. Further, the unpaired t-test was used for two samples which are not related to each other.²⁹ This testing was performed on the three independent groups viz. s-IMRT, d-IMRT and VMAT, and for each group the measurement was performed twice, first by 2D array (PTW, Freiburg) and second by a-Si EPID. The analysis of variance (ANOVA) was used to compare the means of different groups (≤ 2) of data: three groups were s-IMRT, d-IMRT and VMAT. The comparison was done using ANOVA independently for each of the groups between

δ_{IC} , Δ_{Array} and Δ_{EPID} measurements. ANOVA is a statistical technique that characterizes the data in groups and compares the mean and variance of the data among the categories.²⁹ p-values of the distribution were used to evaluate the statistical significance of difference invariability in data between the different categories. In order to identify the differences the means of two or more groups at a time, the method is utilized to interpret and confirm the results of ANOVA. For comparison between the measurements we used software Prism version 6 from GraphPad and $p \leq 0.05$ was considered as significant.

The newest approach of data analysis is based on the applied concepts of statistical process control (SPC). It is commonly used in engineering and industrial applications to proactively monitor the process performance and also helps in focusing on the continuous improvement in the process. Control charts are amongst the quality control tools for SPC to monitor process variation. There are three types of charts: \bar{X} , \bar{S} and EWMA. The \bar{X} chart consists of an upper control (UCL), centre line (CL), lower control limit (LCL) and the data points. The LCL and UCL are usually set at a distance of standard deviations (σ) above and below the CL, the average of the process. The first 50 data points from array $\gamma_{\% < 1}$ and EPID $\gamma_{\% < 1}$ were used to evaluate all the control limits as

$$UCL = \bar{X} + 3 \frac{\overline{MR}}{d_2}$$

$$LCL = \bar{X} - 3 \frac{\overline{MR}}{d_2}$$

$$CL = \bar{X}$$

Where, MR is the value between two consecutive points of percentage (%) of gamma pass ($MR_i = |\Delta_i - \Delta_{i-1}|$). Δ is the average of % difference in gamma pass and \overline{MR} is the average of moving-range of % difference in gamma pass in the subgroup. The constant d_2 depends on the total number of (n) in subgroup. In the present case, n is equal to 2, so d_2 is 1.128.²⁹⁻³⁰ The percentage (%) differences in gamma pass of s-IMRT, d-IMRT and VMAT QA plans measured by 2D-Array ($\gamma_{\% < 1}$) and a-Si EPID ($\gamma_{\% < 1}$) were plotted on control charts for the individual patients. The \bar{X} chart considers each patient's quality control result as an individual value of the QA process. Although \bar{X} charts are widely used, but to determine the process variability or standard deviation(s) graphically, the \bar{S} charts are utilized. The baseline values for the \bar{S} chart were again derived from the 50 control group patients. The control limits were evaluated as

$$UCL = \bar{s} + 3 \left(\frac{\bar{s}}{c_4} \right) \sqrt{1 - c_4^2}$$

$$LCL = \bar{s} - 3 \left(\frac{\bar{s}}{c_4} \right) \sqrt{1 - c_4^2}$$

$$CL = \bar{s}$$

The \bar{s} is the average standard deviation of the sample, c_4 is the function of available groups under consideration. The value of c_4 can be determined from the standard tables available in textbooks.²⁹⁻³⁰ In the present study, for the specific type of radiotherapy delivery the measurements from two detectors 2D Array (PTW, Freiburg) and a-Si EPID were compared. The value of c_4 was taken as 0.7979. \bar{X} and \bar{S} charts are the first phase tools where the process is under the establishment and is experiencing assignable causes for variation. But after the satisfactory implementation of the process, the \bar{X} and \bar{S} charts become relatively insensitive to small process shifts ($< \pm 1.5 \sigma$). In order to monitor the process quality and performance in the long run, the exponentially weighted moving averages (EWMA) type of control chart proves to be useful.²⁹⁻³⁰ A EWMA chart is the time-weighted control chart, it weighs the sample in geometrically decreasing order so that the most recent sample are weighted most highly while the most distant sample contribute very little. The design parameters of the EWMA control chart are

$$z_i = \lambda x_i + (1 - \lambda) z_{i-1}$$

Where, z_i is the exponentially weighted moving average, λ is an age of the sample and with value between 0 and 1. The starting value of λ was taken as 0.3.³⁵ z_i in the beginning $z_0 = \bar{X}$.

$$UCL = \mu_0 + Ls \sqrt{\frac{\lambda}{(2 - \lambda)} [1 - (1 - \lambda)^{2i}]}$$

$$LCL = \mu_0 - Ls \sqrt{\frac{\lambda}{(2 - \lambda)} [1 - (1 - \lambda)^{2i}]}$$

$$CL = \mu_0$$

Where μ_0 is the mean of the preliminary data taken as the starting value, L is the width of the control limit. The value of L was taken as 3.³¹

Process capability analysis is a quantitative method of analyzing the process stability and capability in overall quality management program. This index (C_{pm}) is the measure of process performance within the specification limits. Fundamentally, capability indexes are used to estimate the competence between the production tool and the quality targeted for the product. In radiotherapy scenario, the production refers to a-Si EPID as a detector tool and the product refers the gamma value obtained as the result of patient specific quality assurance activity. It accounts for the data dispersion and determines the closeness of the data (\bar{X}) to the process mean (T). C_{pm} takes into account for both the proximity of process to the target value as well as the magnitude of the process variation.²⁵ It is given as

$$C_{pm} = \frac{USL - LSL}{6\sqrt{\sigma^2 + (\bar{X} - T)^2}}$$

Where, (USL - LSL) is the difference between the upper and lower specification clinical limit, σ^2 is the variance, \bar{X} is the process mean and T is the target value of the process. T is 0%

because the target for the QA process is 100% matching of fluence. The C_{pm} value greater than and equal to 1.33 indicate that the process is operating optimally.³³ The higher the of C_{pm} , the higher is the efficiency of the process. This is due to the fact that the loss function³⁴ appears in the as $\sqrt{\sigma^2 + (\bar{X} - T)^2}$.

Results

Array and EPID based two dimensional measurements had the mean gamma pass rates as $99.9\% \pm 0.15\%$ and $98.9 \pm 1.06\%$ respectively. **Table 1** provide the details of complete sample of 250 plans for different radiotherapy techniques viz. s-IMRT, d-IMRT and VMAT. For the point dose measurements, the ion chamber results were found to be within $2.1\% \pm 0.5\%$ of the central chamber of the array. Similarly, the central axis point doses from EPID and ion chamber matched within $1.5\% \pm 0.3\%$.

TABLE: Summary of the conventional statistics for s-IMRT, d-IMRT & VMAT.

S.N	Parameter	s-IMRT	d-IMRT	VMAT
1	Total no. of plans	250	250	250
2	Total no. of beams/arcs	1750	1793	263
3	Total no. of segments/ports	189548	151258	114190
4	Total no. of monitor units	989731	866354	912850
5	Mean of $\Delta_{Array}(\%)$	1.225	1.29	1.2592
6	Standard deviation of $\Delta_{Array}(\%)$	0.884	0.962	0.978
7	Mean of $\Delta_{EPID}(\%)$	1.27	1.15	1.2662
8	Standard deviation of $\Delta_{EPID}(\%)$	0.912	0.199	0.148

The Jarque-Bera (JB) statistics were implemented for all three techniques; the measurements for Δ_{Array} and Δ_{EPID} were distributed normally.

The **Table 2** illustrates skewness and kurtosis for the three samples. For 1500 plans, a-Si EPID, detector array measured and planning system calculated photon fluence agrees within the action level limits. The observed mean \pm standard deviation values for the gamma analysis were $^{EPID}\gamma_{mean} = 0.81 \pm 0.06$, $^{EPID}\gamma_{max} = 1.46 \pm 0.78$ and $^{EPID}\gamma_{\% \leq 1} = 99.66 \pm 1.54$ and $^{array}\gamma_{mean} = 0.7 \pm 0.05$, $^{array}\gamma_{max} = 1.3 \pm 0.08$ and $^{array}\gamma_{\% \leq 1} = 98.56 \pm 1.29$. Among all the plans γ_{max} was found to be consistently lower in array than a-Si EPID. It was seen that the variation of γ_{max} and $\gamma_{\% \leq 1}$ estimated from array and a-Si EPID for VMAT was 5.6% and 2.4% plans, respectively. However, the variation in γ_{mean} was seen only in 1% cases. The highest values of $\gamma_{\% \leq 1}$ was observed in VMAT plans when measured using a-Si EPID. For 1500 plans, EPID measurements had higher γ_{mean} than the array measurements. The statistical analysis for γ -evaluation

performed using array and EPID with ANOVA showed the average of γ values do not differ much from each other. Thus, it implies that there are no significant differences among the performance of array and EPID. The unpaired t-test for these measurements performed by a-Si EPID and array for s-IMRT, d-IMRT and VMAT were assessed independently and individually. Results indicate that within all the individual groups there were no statistically significant differences observed with $p > 0.05$ in each group. The performances of both the detectors were seen to be of high quality irrespective of the radiotherapy techniques.

In order to assess the variability of the patient specific quality assurance processes for s-IMRT, d-IMRT and VMAT for the measurements performed by array and a-Si EPID, the concepts of statistical process control (SPC) were also implemented using \bar{X} , \bar{S} and EWMA control charts. The CL, UCL and LCL of the \bar{X} chart were evaluated from first 50 cases for analyzing 250 s-IMRT, d-IMRT and VMAT for both the array and a-Si EPID measurements. The value of UCL has been fixed to 100% because it is the maximum value for $\gamma < 1$. The \bar{X} charts are presented in **Figure 1(a-c)** for s-IMRT, d-IMRT and VMAT. The \bar{S} charts were also generated for the collected data to monitor the process variability over time.

The \bar{S} charts are presented in **Figure 2(a-c)** for s-IMRT, d-IMRT and VMAT. The EWMA charts were also generated to monitor the variability in the process mean over a particular period. The performance of the process can be reviewed weekly to find out the trends or drifts in process. EWMA chart is sensitive even lesser than 1.5σ level variation. The EWMA charts are presented in **Figure 3**. The smooth trend was observed in all the processes for present study indicating the processes were found well within the control limits. Like conventional statistical analysis results, the CC analysis was also suggestive of the fact that for all the advanced radiotherapy techniques both array and a-Si EPID based planar measurements were performing optimally.

Another approach of evaluating the capability indices was applied to the collected data. The values of this index are mentioned in **Table 2**. The values of this index for all the different combinations were found to be < 1.33 , which ensures a good level of quality for the processes. For all the measurements performed with a-Si EPID, irrespective of radiotherapy technique, obtained a better and higher value of C_{pm} . It was also seen that the highest value of C_{pm} was obtained for the combination of VMAT QA plans measured using a-Si EPID.

TABLE 2: Mean $\pm 1.96\sigma$ of $\gamma\%$ pass, Skewness, Kurtosis and capability index C_{pm} for the array and a-Si EPID measurements for s-IMRT, d-IMRT and VMAT

	VMAT		d-IMRT		s-IMRT	
	EPID	Array	EPID	Array	EPID	Array
Mean ($\gamma\%$ pass)	98.64	98.58	98.53	98.47	98.68	98.55
Standard deviation (σ) ($\gamma\%$ pass)	1.18	1.20	1.28	1.22	1.38	1.29
No. of patients in the range Mean $\pm 1.96\sigma$	248.0	239.0	246.0	235.0	237.0	236.0
% of patients in the range mean $\pm 1.96\sigma$	99.20	95.60	98.40	94.00	94.80	94.40
Skewness	0.49	0.51	0.67	0.58	0.77	0.75
Kurtosis	-0.88	-0.78	-0.26	-0.49	-0.43	-0.25
Normality Test	Pass	Pass	Pass	Pass	Pass	Pass
C_{pm} values	1.55	1.45	1.58	1.46	1.57	1.43

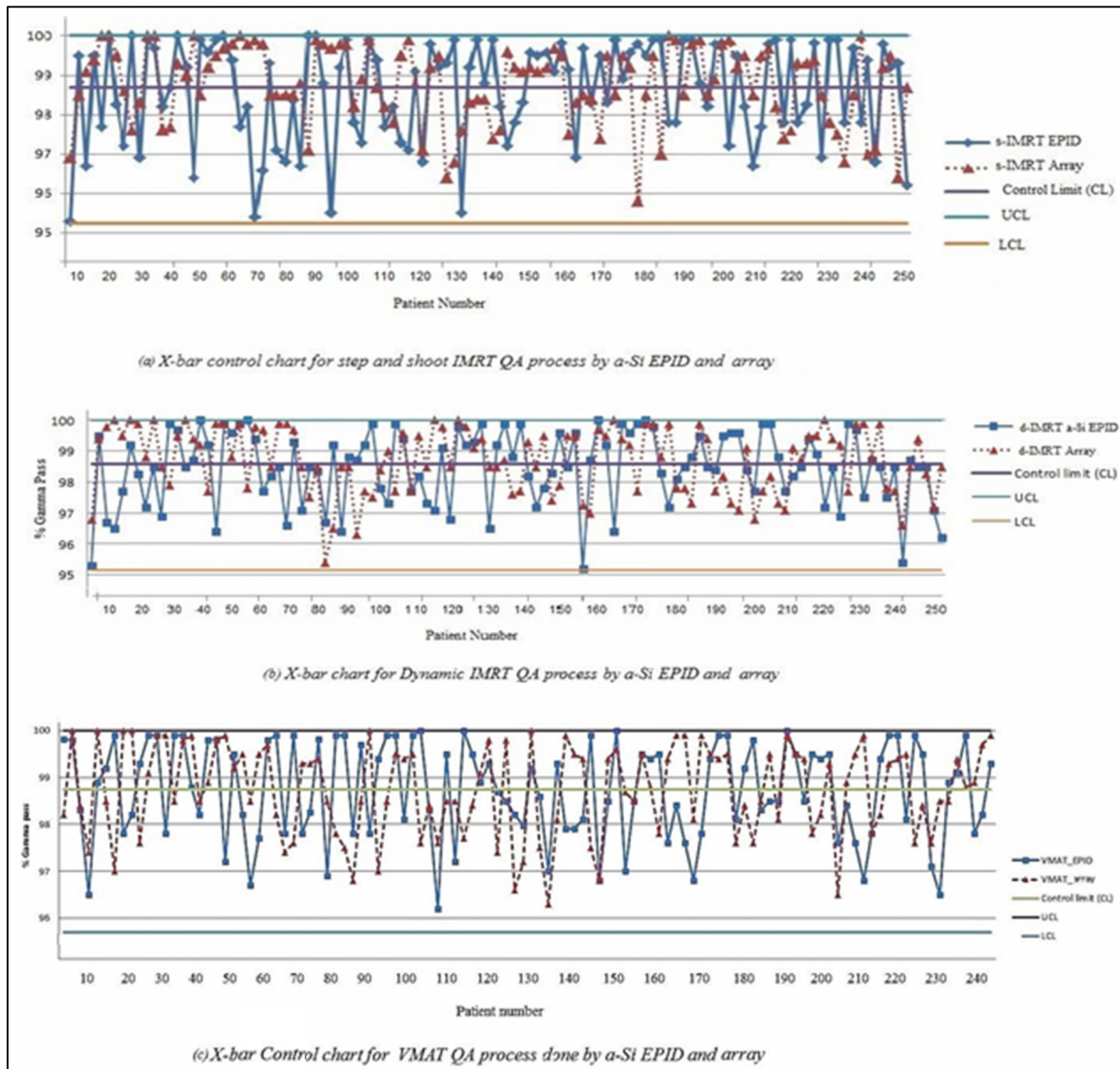


FIG. 1(a-c): \bar{X} control charts for s-IMRT, d-IMRT and VMAT QA measurements by a-Si EPID and array

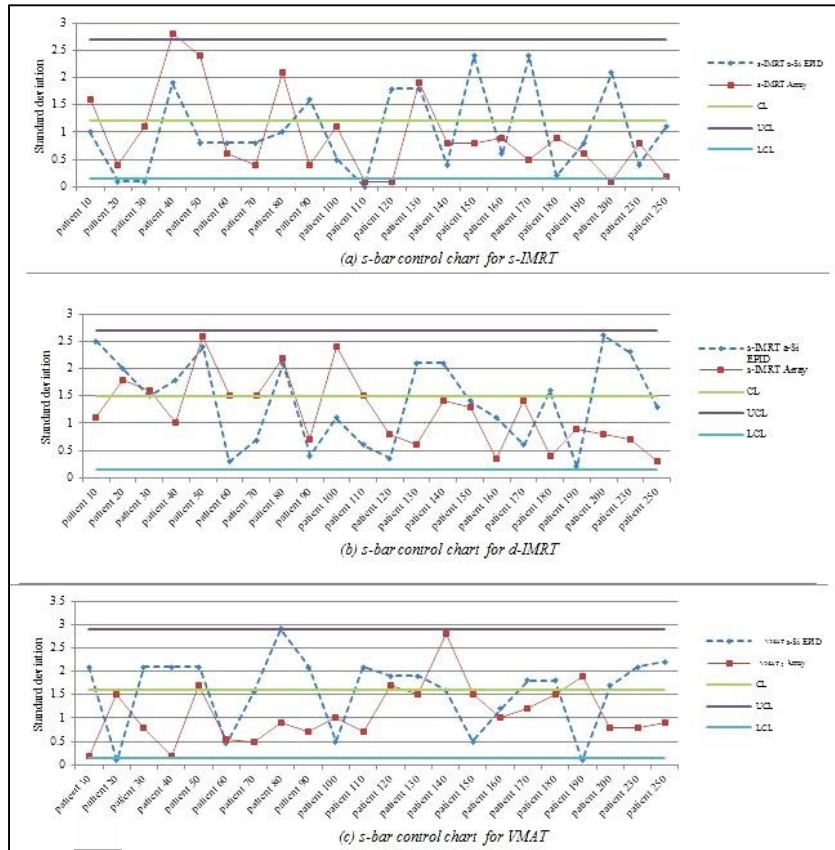


FIG. 2(a-c): \bar{s} control charts for s-IMRT, d-IMRT and VMAT QA measurements by a-Si EPID and array

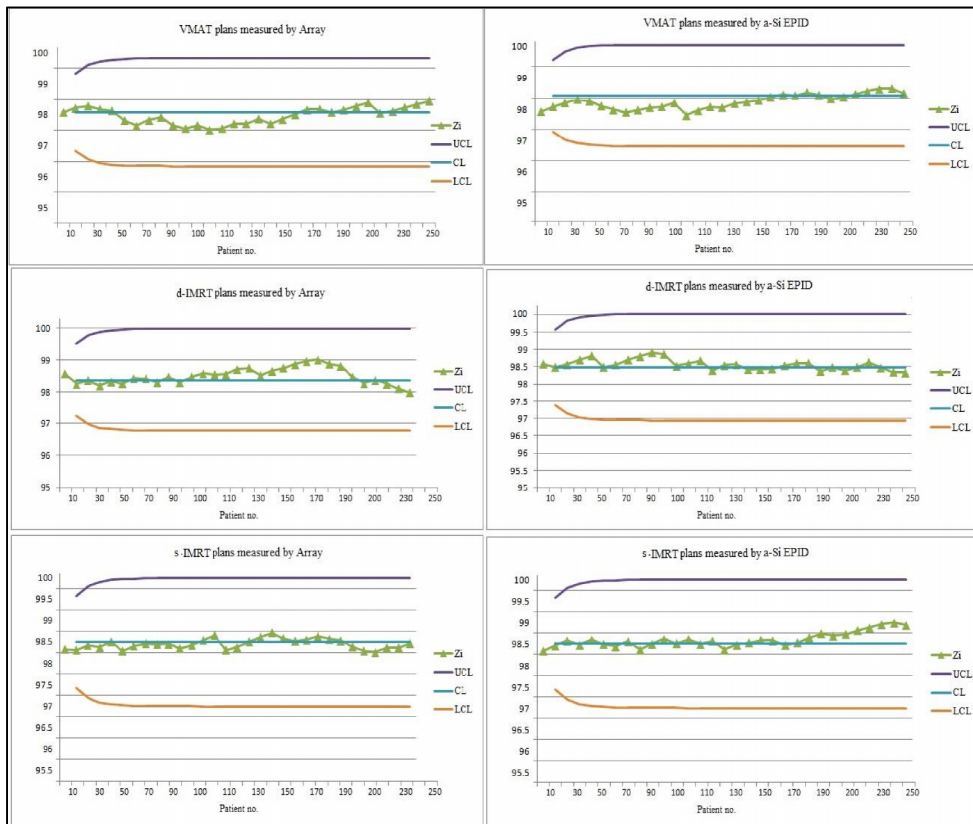


FIG. 3: EWMA control charts for s-IMRT, d-IMRT and VMAT QA measurements by a-Si EPID and array

Discussion

The complex planning and timely response of the extensive hardware in the modern radiotherapy techniques has made patient specific QA a standard of practice.¹⁰ In our institute, the pre-treatment verification of the s-IMRT, d-IMRT and VMAT plans have been carried out using ion chamber array and a-Si EPID routinely. The array is calibrated for measuring absolute dose using standard field size (10 cm × 10 cm for Synergy and 10.4 cm × 10.4 cm for Axesse) and routinely evaluates the agreement between TPS calculated and ion chamber array measured dose. Portal dosimetry as a pre-treatment QA tool for advanced radiotherapy techniques is in its infancy although few centers have been using it mostly with their indigenously developed software.^{22,35-37} In the present work the a-Si EPID captured fluence was normalized with the computed data at the isocentric pixel for cGy conversion in verisoft software (PTW, Freiburg). This normalized fluence was then compared with the calculated fluence at couch level on the 5 cm thick water equivalent slab phantom. We are reporting array and a-Si EPID comparative results for s-IMRT, d-IMRT and VMAT using PTW Verisoft software for gamma analysis. Our results shows very good agreement between calculated and measured dose distribution in all plans with overall mean ± SD gamma values as shown in **Table 2**. Recently, portal dosimetry results from Varian were reported from Howell.²² The authors reported the results from 152 IMRT plans that the overall mean ± SD $\gamma_{\max} = 2.4 \pm 0.8$, $\gamma_{\text{avg}} = 0.33 \pm 0.13$ and $\gamma_{\% > 1} = 4.1\% \pm 6.2\%$. Also, for complex head and neck planning, Howell *et al.* has reported higher gamma values. Our results are in agreement with this study.

The advantage of control charts is that it is instrumental in accessing the performance of the process/equipment over the time and also facilitating the user to identify the causative factor of variation in the process/equipment. Originally, control charts are employed in the industrial applications to maintain the quality of each individual product but the similar concept can be extended to the radiation oncology services.¹⁸ With the implementation of such a concept in radiation oncology, there will be a paradigm shift towards improvement in patient care. For the advanced technologies in radiation therapy, the minimum requirement is to ensure their dosimetric accuracy and needs to be determined for every patient individually. Pawlicki^{14, 15} have identified the utilization of control charts for monitoring the performance of linear accelerator for the measurements of output and beam characteristics (flatness and symmetry) for 10 MV photon beam. Gerard¹⁶ have studied total 119 dynamic IMRT head and neck and prostate cases retrospectively, and have shown the usage of all three types of control charts and performance linked indices for point dose measurements.

The overall results of patient-specific QA for advanced radiotherapy techniques using array and a-Si EPID are comparable to each other. The γ measurements using a-Si EPID produced higher results than array. The charts also graphically illustrated that all the processes were performing optimally. The statistical reliability of the detectors in advanced radiotherapy techniques was determined using C_{pm} index. The C_{pm} values imply that all the QA processes irrespective of the techniques and detector choice were performing optimally. Higher the value of $C_{\text{pm}} < 1.33$, the efficient is the performance of the equipment. The a-Si EPID based dosimetry process obtained higher value of C_{pm} than that of the detector array.

Conclusion

a-Si based EPID and array were found to be consistent in quality performance for modern radiotherapy dosimetry. Higher values for $^{EPID}C_{\text{pm}}$ indicate higher statistical reliability and efficiency for EPID than the array based measurements. Statistical process control is realized as the scientific and pictorial way of analyzing the real time data and simultaneously provides the immediate feedback for the newer incoming data points derived from quality assurance results of s-IMRT/d-IMRT/VMAT.

Acknowledgement

The authors would like to thank Mr. Tushar KY and Ms. Veena Viswambharan B who provided technical support and assistance during the performance and data collection of this work.

Conflict of interest

The authors declare that they have no conflicts of interest. The authors alone are responsible for the content and writing of the paper.

References

1. Li XA, Wang JZ, Jursinic PA, *et al.* Dosimetric advantages of IMRT simultaneous integrated boost for high-risk prostate cancer. *Int J Radiat Oncol Biol Phys* 2005; **61**:1251-7.
2. Cilla S, Macchia G, Digesù C, *et al.* 3D-Conformal versus intensity-modulated postoperative radiotherapy of vaginal vault: A dosimetric comparison. *Med Dosim* 2010; **35**:135-42.
3. Bucci MK, Bevan A, Roach M 3rd. Advances in radiation therapy: conventional to 3D, to IMRT, to 4D, and beyond. *CA Cancer J Clin* 2005; **55**:117-34.
4. Alvarez-Moret J, pohl F, Koeibl O, *et al.* Evaluation of Volumetric modulated arc therapy (VMAT) with

- Oncentra MasterPlan® for the treatment of head and neck cancer. *Radiat Oncol* 2010; **5**:110.
5. Chao KS, Majhail N, Huang CJ, et al. Intensity-modulated radiation therapy reduces late salivary toxicity without compromising tumor control in patients with oropharyngeal carcinoma: a comparison with conventional techniques. *Radiother Oncol* 2010; **61**:275-80.
 6. Webb S. Intensity-modulated Radiation Therapy. IOP publication, 2002
 7. Otto K. Volumetric modulated arc therapy: IMRT in a single gantry arc. *Med Phys* 2008; **35**: 310-7.
 8. Teoh M, Clark CH, Wood K, et al. Volumetric modulated arc therapy: a review of current literature and clinical use in practice. *Br J Radiol* 2011; **84**: 967-96.
 9. Galvin JM, Ezzell G, Eisbrauch A, et al. Implementing IMRT in clinical practice: a joint document of the American Society for Therapeutic Radiology and Oncology and the American Association of Physicists in Medicine. *Int J Radiat Oncol Biol Phys* 2004; **58**:1616-34.
 10. Van Dyk J, Purdy J. Clinical implementation of technology and the quality assurance process; in *The Modern Technology of Radiation Oncology. Medical Physics*, Madison WI, 1999.
 11. Low DA, Moran JM, Dempsey JF, et al. Dosimetry tools and techniques for IMRT. *Med Phys* 2011; **38**:1313-37.
 12. Low DA, Harms WB, Sasa M, Purdy JA. A technique for the quantitative evaluation of dose distributions. *Med Phys* 1998; **25**:1919-27.
 13. Depuydt T, Van Esch A, Huyskens DP. A quantitative evaluation of IMRT dose distributions: refinement and clinical assessment of the gamma evaluation. *Radiother Oncol* 2002; **62**:309-19.
 14. Pawlicki T, Whitaker M, Boyer AL. Statistical process control for radiotherapy quality assurances. *Med Phys* 2005; **32**:2777-86.
 15. Pawlicki T, Yoo S, Court LE, et al. Moving from IMRT QA measurements toward independent computer calculations using control charts. *Radiother Oncol* 2008; **89**:330-7.
 16. Gerad K, Grandhaye JP, Marchesi V, et al. A comprehensive analysis of the IMRT dose delivery process control (SPC). *Med Phys* 2009; **36**:1275-85.
 17. Breen SI, Moseley DJ, Zhang B, et al. Statistical process control for IMRT dosimetric verification. *Med Phys* 2008; **35**:4417-25.
 18. Thomadsen BR, Dunscombe P, Ford E, et al. Quality and Safety in Radiotherapy: Learning the New Approaches in Task Group 100 and Beyond, AAPM Monograph #36, Medical Physics Publication, **2013**.
 19. Gagneur JD, Ezzell GA. An improvement in IMRT QA results and beam matching in linacs using statistical process control. *J Appl Clin Med Phys* 2014; **15**:4927.
 20. Acquah GF, Gustavsson M, Doudoo CO, et al. Clinical use of electronic portal imaging to analyze tumor motion variation during a 3D-conformal prostate cancer radiotherapy using online target verification and implanted markers. *Int J Cancer Ther Oncol* 2014; **2**:02044.
 21. Stanley DN, Papanikolaou N, Gutierrez AN. An evaluation of the stability of image quality parameters of Varian on-board imaging (OBI) and EPID imaging systems. *Int J Cancer Ther Oncol* 2014; **2**:020236.
 22. Howell RM, Smith IP, Jarrio CS. Establishing action levels for EPID-based QA for IMRT. *J Appl Clin Med Phys* 2008; **9**:2721.
 23. Rout BK, Shekar MC, Kumar A, Ramesh KKD. Quality control test for electronic portal imaging device using QC-3 phantom with PIPSPRO. *Int J Cancer Ther Oncol* 2014; **2**:02049.
 24. Jassal K, Munshi A, Sarkar B, et al. Validation of an integrated patient positioning system: Exactrac and iViewGT on Synergy Platform. *Int J Cancer Ther Oncol* 2014; **2**:020212.
 25. Kawrakow I, Fippel M, Friedrich K. 3D electron dose calculation using a Voxel based Monte Carlo algorithm (VMC). *Med Phys* 1996; **23**:445-57.
 26. Fippel M, Laub W, Huber B, Nüsslin F. Experimental investigation of a fast Monte Carlo photon beam dose calculation algorithm. *Phys Med Biol* 1999; **44**:3039-54.
 27. Jarque CM, Bera AK. A Test for Normality of Observations and Regression Residuals. *International Statistical Review* 1987; **55**: 163-72.
 28. Kothari CR, Research Methodology: Methods and Techniques; Wiley Eastern Limited, New Delhi, 2006.
 29. Wheeler DJ, Chambers D S, Understanding Statistical Process Control, 2nd edition; Knoxville SPC press, 1992.
 30. Montgomery DC. Introduction to Statistical Quality Control; Wiley, New York, 2004
 31. Lucas JM, Saccucci MS. Exponentially weighted moving averages control schemes: Properties and enhancements. *Technometrics* 1990; **32**:1-29.
 32. Chan LK, Cheng SW, Spiring FA. A new measure of process capability: Cpm. *Journal of Quality Technology* 1988; **20**:162-75.
 33. Pillet M, Rochon S, Duclos E. SPC- Generalization of capability index Cpm: Case of unilateral tolerances. *Quality Engineering* 1997; **10**: 171-6.
 34. Taguchi G, Elsayed A. E and Hsiang T. Quality Engineering in production systems, McGraw Hill, New York, 1989.
 35. Van Esch A, Depuydt T, Huyskens DP. The use of an aSi-based EPID for routine absolute dosimetric

- pre-treatment verification of dynamic IMRT fields. *Radiother Oncol* 2004; **71**:223-34.
36. McDermott LN, Wendling M, van Asselen B, *et al*. Clinical experience with EPID dosimetry for prostate IMRT pre-treatment dose verification. *Med Phys* 2006; **33**:3921-30.
37. van Zijtveld M, Dirkx MLP, de Boer HC, Heijmen BJ. Dosimetric pre-treatment verification of IMRT using an EPID; clinical experience. *Radiother Oncol* 2006; **81**:168-75.